Guanylate cyclase promotes osseointegration by inhibiting oxidative stress and inflammation in aged rats with iron overload

From The First Affiliated Hospital of Wannan Medical College, Wuhu, China

Z-S. Tao,[1,2] C-L. Shen[3]

[1]Department of Orthopedics, The First Affiliated Hospital of Wannan Medical College, Yijishan Hospital, Wuhu, China
[2]Anhui Province Key Laboratory of Non-coding RNA Basic and Clinical Transformation, Wuhu, China
[3]Department of Spinal Surgery, The First Affiliated Hospital of Anhui Medical University, Hefei, China

Cite this article:
Bone Joint Res 2024;13(9):
427–440.

DOI: 10.1302/2046-3758.
139.BJR-2023-0396.R3

Correspondence should be sent to Cai-Liang Shen
SCL20231990@126.com

Aims

This study intended to investigate the effect of vericiguat (VIT) on titanium rod osseointegration in aged rats with iron overload, and also explore the role of VIT in osteoblast and osteoclast differentiation.

Methods

In this study, 60 rats were included in a titanium rod implantation model and underwent subsequent guanylate cyclase treatment. Imaging, histology, and biomechanics were used to evaluate the osseointegration of rats in each group. First, the impact of VIT on bone integration in aged rats with iron overload was investigated. Subsequently, VIT was employed to modulate the differentiation of MC3T3-E1 cells and RAW264.7 cells under conditions of iron overload.

Results

Utilizing an OVX rat model, we observed significant alterations in bone mass and osseointegration due to VIT administration in aged rats with iron overload. The observed effects were concomitant with reductions in bone metabolism, oxidative stress, and inflammation. To elucidate whether these effects are associated with osteoclast and osteoblast activity, we conducted in vitro experiments using MC3T3-E1 cells and RAW264.7 cells. Our findings indicate that iron accumulation suppressed the activity of MC3T3-E1 while enhancing RAW264.7 function. Furthermore, iron overload significantly decreased oxidative stress levels; however, these detrimental effects can be mitigated by VIT treatment.

Conclusion

Collectively, our data provide compelling evidence that VIT has the potential to reverse the deleterious consequences of iron overload on osseointegration and bone mass during ageing.

Article focus

- The purpose was to observe the effect of vericiguat (VIT) on osseointegration in aged rats with iron overload, and also to explore the role of VIT in osteogenic differentiation of MC3T3-E1 cells and RAW264.7 cells.

Key messages

- This study found that VIT has the potential to reverse the deleterious consequences of iron overload on osseointegration and bone mass during ageing.

Strengths and limitations

- We investigated for the first time the adverse effects of iron overload on osseointegration, and explored the ability of guanylate cyclase to reverse the adverse effects of iron overload.
- The specific mechanism behind VIT was not investigated, therefore further research is needed.

Introduction

Osteoporosis is the most common metabolic skeletal disorder, characterized by reduced bone mineral density which results in the destruction of bone microstructure and damage to bone structure.[1] In recent years, the prevalence of osteoporosis has been increasing persistently.[2,3] With ageing, the probability of injury through various causes increases, especially through the risk of falling.[4] Over the past few decades, with the rapid and innovative advances in treatment and surgery, and the emergence of new internal fixation equipment, orthopaedic surgery has gained widespread acceptance and become the first choice for osteoporotic fracture patients.[5,6] Commonly, a stronger anchorage of implants into bone is a key factor that determines the success of such orthopaedic implants, referred to as osseointegration.[5] Additionally, the bone-implant interface must possess both quality and quantity to establish a connection between the implant and bone tissue, thereby promoting osseointegration.[7,8] However, low-quality bone and persistent bone mass loss may lead to failed osseointegration of the implant.[9,10] Therefore, removing disruptions to bone metabolism can be of great value to aid long-term effective osseointegration, and is therefore a potential strategy for reducing implant loosening.

Iron is a unique trace element and contributes to important diverse biological processes such as oxygen transport, electron transport, signal transduction, and DNA synthesis.[11] Iron homeostasis is precisely regulated by the control of iron absorption and uptake,[12] and abnormal iron metabolism can lead to toxic side effects.[13] Maintaining physiological iron homeostasis is critical for normal organism and cell metabolism and function, and abnormal iron metabolism has been implicated in a variety of diseases, such as cardiovascular disease.[14] One study has established that altered iron metabolism is closely related to the initiation and progression of bone loss.[15] It has been reported that iron overload can cause increased levels of oxidative stress and inflammation in tissues and organs, which can lead to impaired bone formation and increased bone resorption, resulting in imbalance of bone remodelling and increased risk of bone loss and fracture.[16] One recent study has suggested that activation of guanylate cyclase activity modulates osteoclast differentiation and bone resorption.[17] It has also been reported that activation of guanylate cyclase activity can promote osteogenic differentiation and increase osteogenic activity through nitric oxide-soluble guanylate cyclase-cyclic guanylic acid (NO-SGC-CGMP) signalling cascade.[18] Vericiguat (VIT), an oral drug approved by the US Food and Drug Administration in 2021 to treat heart failure,[19] increases soluble guanylate cyclase activity and activates the NO-SGC-CGMP pathway.[20] Due to its anti-inflammation and antioxidative stress properties, VIT can improve the survival rate of patients with heart failure and reduce hospitalization and mortality.[21] Considering the antioxidative stress and anti-inflammatory effects of VIT, as well as the detrimental impact of iron overload on bone health due to elevated levels of oxidative stress and inflammation, a plausible hypothesis can be proposed: VIT may have the potential to mitigate bone damage caused by iron overload. However, whether VIT can resist the adverse effects of iron overload on osseointegration remains ambiguous.

Although great advances have been made in understanding iron overload-induced oxidative stress in recent years, whether VIT can be beneficial for osseointegration with iron overload is still unknown. Therefore, in this study, we used 24-month-old male Sprague-Dawley (SD) rats as experimental animal subjects, with titanium rods implanted in both femora and treated with VIT based on iron overload, to explore changes in osseointegration, and conducted a preliminary exploration of possible mechanisms through cellular experiments.

Methods

Animals, surgery, and treatment

This study was approved by the Institutional Animal Care and Use Committee of Wannan Medical College, and we have included an ARRIVE checklist to show that we have conformed to the ARRIVE guidelines.

Aged male SD rats (24 months old, n = 45), weighing 500 to 550 g, and young male SD rats (3 months old, n = 15), weighing 220 to 250 g, were used for this study. The animals were raised in a standard laboratory animal room with controlled conditions (temperature 20°C ± 3°C, humidity 45% ± 5%). A resource equation method was used to determine sample size and justify the number of animals, in accordance with previous studies as detailed in the Supplementary Material.[22,23] Animals were randomly divided into four experimental groups: control (Con) (n = 15 young rats), ferric ammonium citrate (FAC) (n = 15 aged rats), lower Verciguat (LVIT) + FAC (n = 15 aged rats), and higher VIT (HVIT) + FAC (n = 15 aged rats). Afterwards, the titanium rods (Shandong Pfizilai Biological Engineering, China), characterized by a length of 20 mm and a diameter of 1.2 mm, were inserted in the left side of the rats according to previous studies.[24,25] Briefly, the animals were anaesthetized with 2% pentobarbital sodium (50 mg/kg) and placed in the prone position, the hair of the left lateral condyle was removed, and the skin was disinfected. The skin and subcutaneous tissue were incised layer by layer until the femoral condyle was exposed. A hole from the lateral femoral condyle to the medial femoral condyle was prepared using a medical slow drill, and a titanium rod was then implanted into the medullary canal through this channel. After the operation, the subcutaneous tissue and wounds were sutured. The rats in the Con group and FAC group were orally treated with isotonic saline and 40 mg/kg FAC, respectively (FAC, Sigma-Aldrich, USA) three times a week, and the animals belonging to the LVIT + FAC and HVIT + FAC groups were orally administered FAC (40 mg/kg, three times a week) plus lower Verciguat (5 μg/kg/day, Sigma-Aldrich) or higher Verciguat (10 μg/kg/day, Sigma-Aldrich), respectively. The doses of FAC and VIT were determined according to a previous experiment.[24,25] At the end of the experiment, all the remaining animals were killed and the femora were obtained, along with blood samples taken after 12 weeks of treatment.

Micro-CT scanning

The femora (the left femur with the titanium rod and the right femur without the titanium rod) were scanned using Micro-CT (Skyscan 1276, Bruker, Belgium), and 3D reconstruction to evaluate the trabecular microstructure and bone formation around the titanium rod in the distal femur was performed. The scanning parameters and matrix size were set at 49 kv,

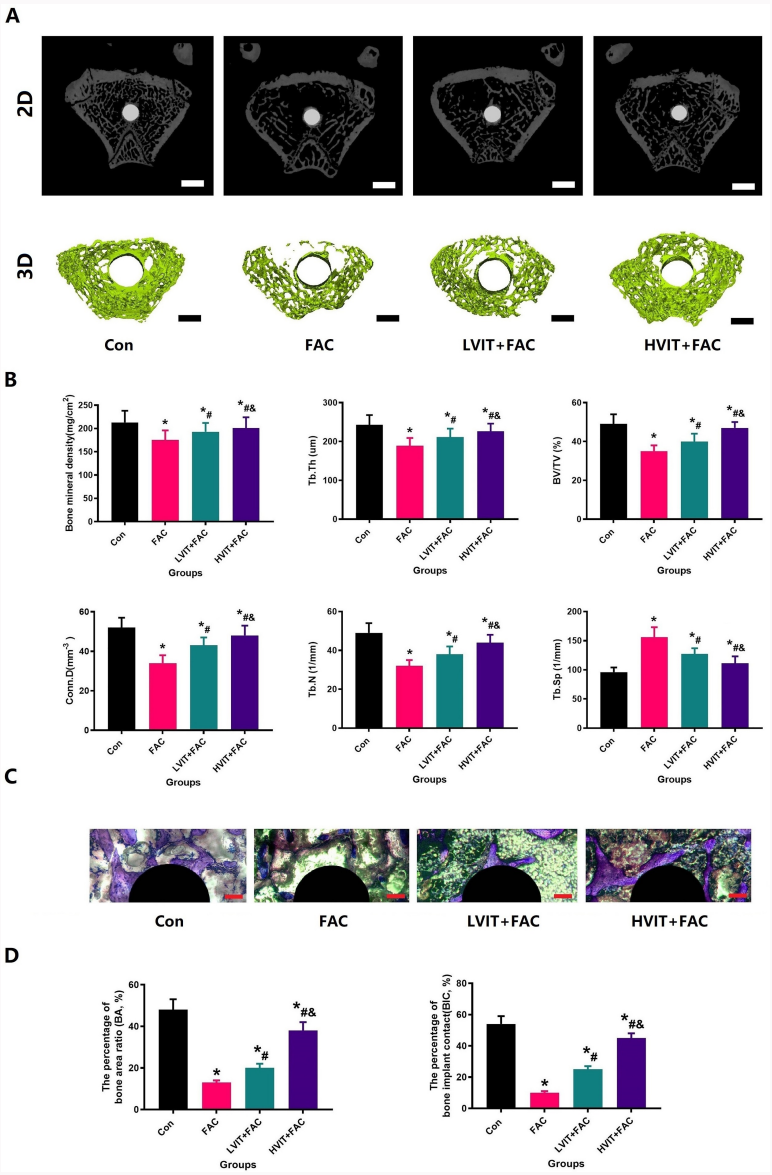

Fig. 1

The impact of vericiguat (VIT) administration on bone formation around the titanium rod in aged rats treated with ferric ammonium citrate (FAC). a) 2D and 3D micro-CT images of the distal femur and surrounding bone tissue obtained from different experimental groups (Con, FAC, lower VIT (LVIT) + FAC, higher VIT (HVIT) + FAC) at a post-implantation period of 12 weeks. The micro-CT images were acquired from a total of 100 transverse slices located approximately 2 mm below the epiphyseal plate of the femur. The scale bar in the images represents a distance of 2 mm. b) Quantitative results derived from micro-CT assessment conducted to evaluate implant osseointegration and peri-implant bone mass 12 weeks post-implantation. c) Transverse histological sections of the distal femur were examined 12 weeks after implant insertion in four different groups: Con, FAC, LVIT + FAC, and HVIT + FAC. All histological sections were taken approximately 2 mm below the epiphyseal plate of the distal femur and stained with toluidine blue Von-Gieson (magnification 10×). d) The bone-implant contact (BIC) and bone area ratio (BAR) were measured after a 12-week period following implantation. There were five specimens per group. * = vs Control group, p = 0.003; # = vs FAC, p = 0.007; & = vs LVIT+ FAC group, p = 0.013. All independent-samples *t*-test and one-way analysis of variance.

200 μA, exposure time 500 ms, 1 mm aluminium filter, and 180° rotation. More than 500 consecutive layers were scanned from the epiphyseal line of the distal femur to the proximal femur. Then, cross-sectional scanned images were analyzed and reconstructed in 3D using CTAn SkyScan software. For evaluation of bone formation around the titanium rod, the central 250 μm-diameter region around the surface of the titanium rod was defined by drawing a circular contour as a consistent volume of interest (VOI). After 3D reconstruction, bone mineral density (BMD), bone mineral content (BMC), bone volume fraction (BV/TV), trabecular number (Tb.N), trabecular thickness (Tb.Th), and trabecular separation (Tb.Sp) were automatically determined for identification of osteoporosis, while BMD, BV/TV, Tb. N, Tb. Th, Tb. Sp, and the mean connective density (Conn.D) in VOI regions were used to evaluate new bone formation, using a protocol provided by the manufacturer of the micro-CT scanner as previously described.[26,27]

Histological examination and immunohistochemical analysis

After the micro-CT evaluation, the femur implanted with titanium rods was dehydrated with alcohol and embedded in polymethyl methacrylate (PMMA). Next, the hardened femora

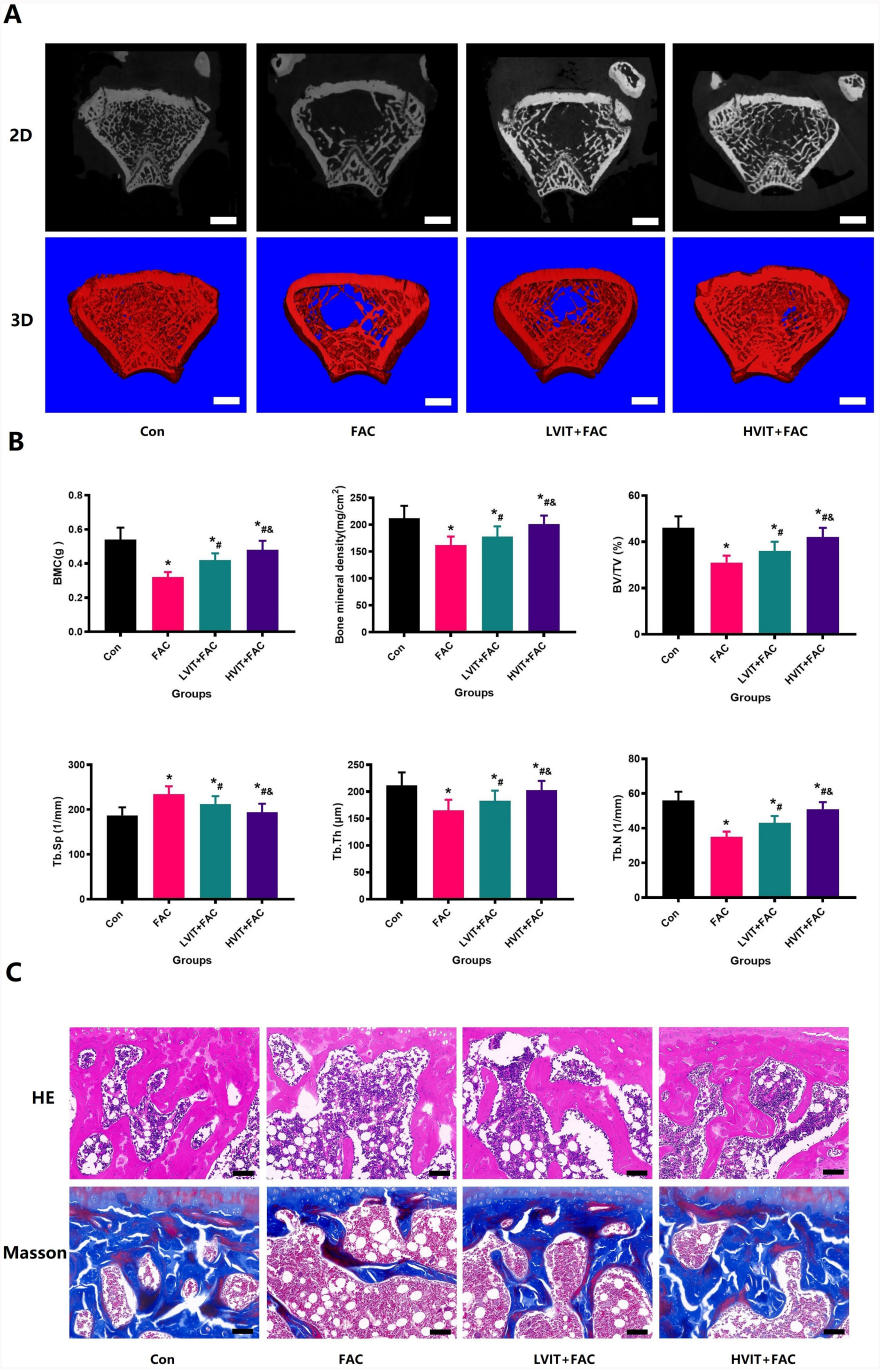

Fig. 2

The impact of vericiguat (VIT) administration on bone mass and bone microstructure in aged rats treated with ferric ammonium citrate (FAC). a) Representative micro-CT images of the femoral metaphysis in different experimental groups (Con, FAC, lower VIT (LVIT) + FAC, higher VIT (HVIT) + FAC), both in 2D and 3D formats. The scale bar corresponds to a length of 1 mm. b) Quantitative outcomes obtained from micro-CT analysis aimed at assessing alterations in microstructural parameters within the distal bone trabeculae of the femur. c) Representative images of haematoxylin and eosin and Masson staining for the femoral metaphysis in various experimental groups, namely Con, FAC, LVIT + FAC, and HVIT + FAC. Scale bar: 100 μm, magnification ×20. There were five specimens per group. * = vs Control group, p = 0.002; # = vs FAC, p = 0.017; & = vs LVIT + FAC group, p = 0.003. All independent-samples *t*-test and one-way analysis of variance.

containing the titanium implant were cut into approximately 200 μm-thick sections along the sagittal axis using a microtome machine (Leica Microsystem), and ground and polished to approximately 50 μm for Von-Gieson staining observation.[28,29]

The femora without titanium rods were decalcified with 10% ethylenediaminetetraacetic acid (EDTA) for four weeks. Then, decalcified femur specimens were embedded in paraffin. Next, the femur specimens were cut into 5 μm slices along the sagittal plane. Next, the sections were dehydrated by using a series of ethanol washes, cleared in xylene, stained with haematoxylin and eosin (HE) or Masson, and mounted with xylene-based mounting medium. HE and Masson staining were conducted to assess the trabecular bone in the distal femur. Stained slides were visualized using a light

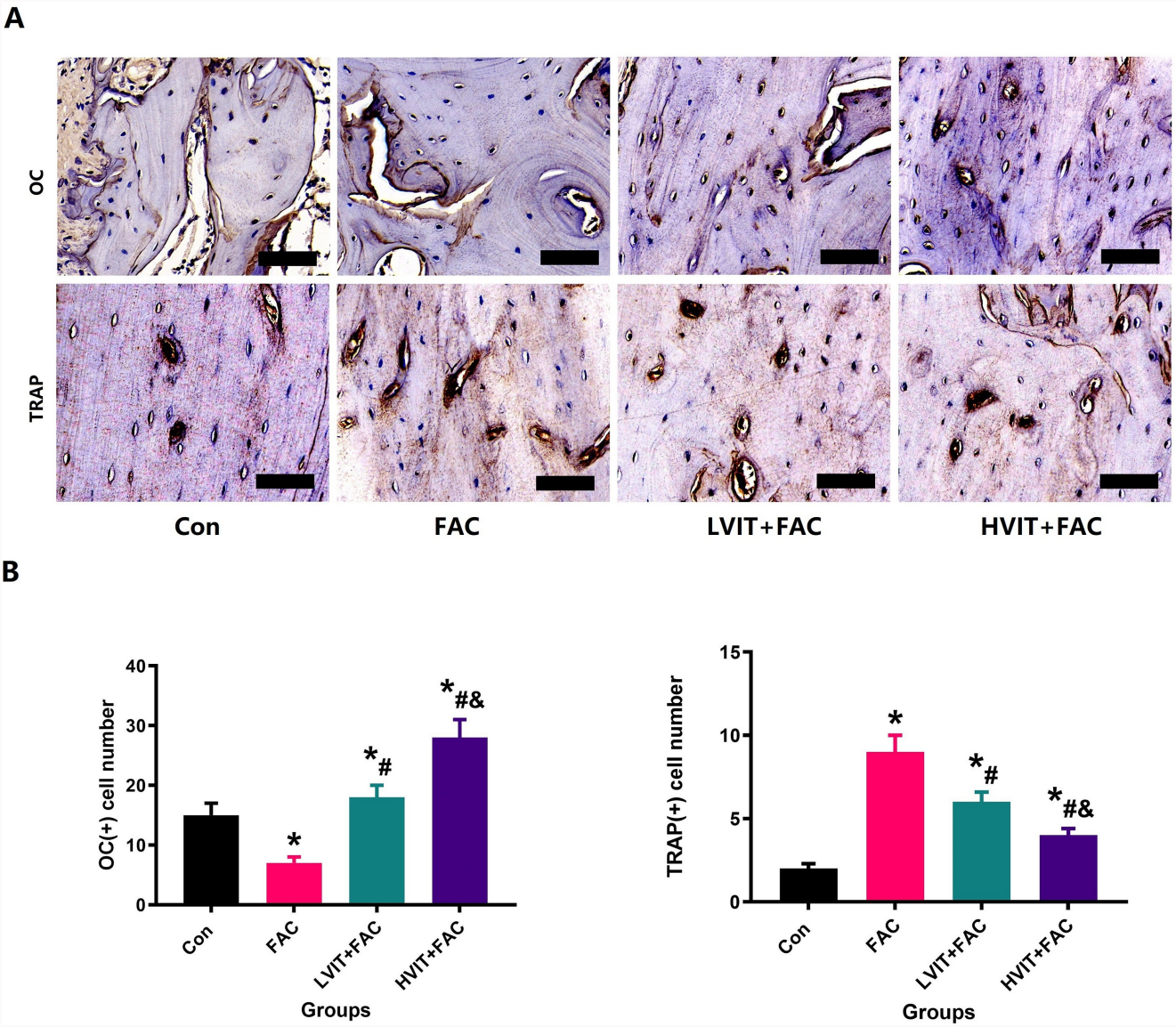

Fig. 3

The impact of vericiguat (VIT) administration on osteoblast and osteoclast activity in aged rats treated with ferric ammonium citrate (FAC). a) Representative images of immunohistochemistry analysis was conducted to assess osteocalcin (OC) and tartrate-resistant alkaline phosphatase (TRAP) levels. Scale bar: 50 μm magnification ×63. b) Quantitative assessment of OC and TRAP was performed. There were five specimens per group. * = vs Control group, p = 0.005; # = vs FAC, p = 0.012; & = vs lower VIT (LVIT) + FAC group, p = 0.007. All independent-samples *t*-test and one-way analysis of variance.

microscope with polarized light capabilities (Eclipse E800; Nikon, Japan).

Immunohistochemistry was further used to evaluate the expression of specific proteins osteocalcin (OC) and tartrate-resistant alkaline phosphatase (TRAP) in bone tissue. In brief, on the basis of the decalcified femur section, the specimens were incubated with rabbit polyclonal antibodies against OC (1:200, Boster Bio (USA), PB1009) and TRAP (1:200, Boster Bio, A14697) overnight. Next, the specimens were also incubated with secondary antibody (1:500, Boster Bio, BA1017). DAB Kit (ZSGB-BIO Corporation, China) was used to develop positive expression. Images were obtained using a biomicroscope (Ni-E, Nikon).

Mechanical testing

The proximal and distal sides of the femur were excised to expose the titanium implants. In particular, it was necessary to expose the distal femur to a 2 mm length of titanium rod for subsequent pull-out experiments. The pull-out tests along the long axis of the rod, including the strength of fixation, energy to failure, and interface stiffness, were measured using a universal testing machine (Instron 4302; Instron, USA) at a constant displacement rate of 0.5 mm/min as previously described.[30,31] The femora without the implant conducted a three-point bending test expressed as energy to failure, ultimate load, and stiffness as previously described.[24]

Biochemical analysis

The levels of bone turnover markers, including procollagen type 1 N-terminal propeptide (P1NP) and carboxy-terminal

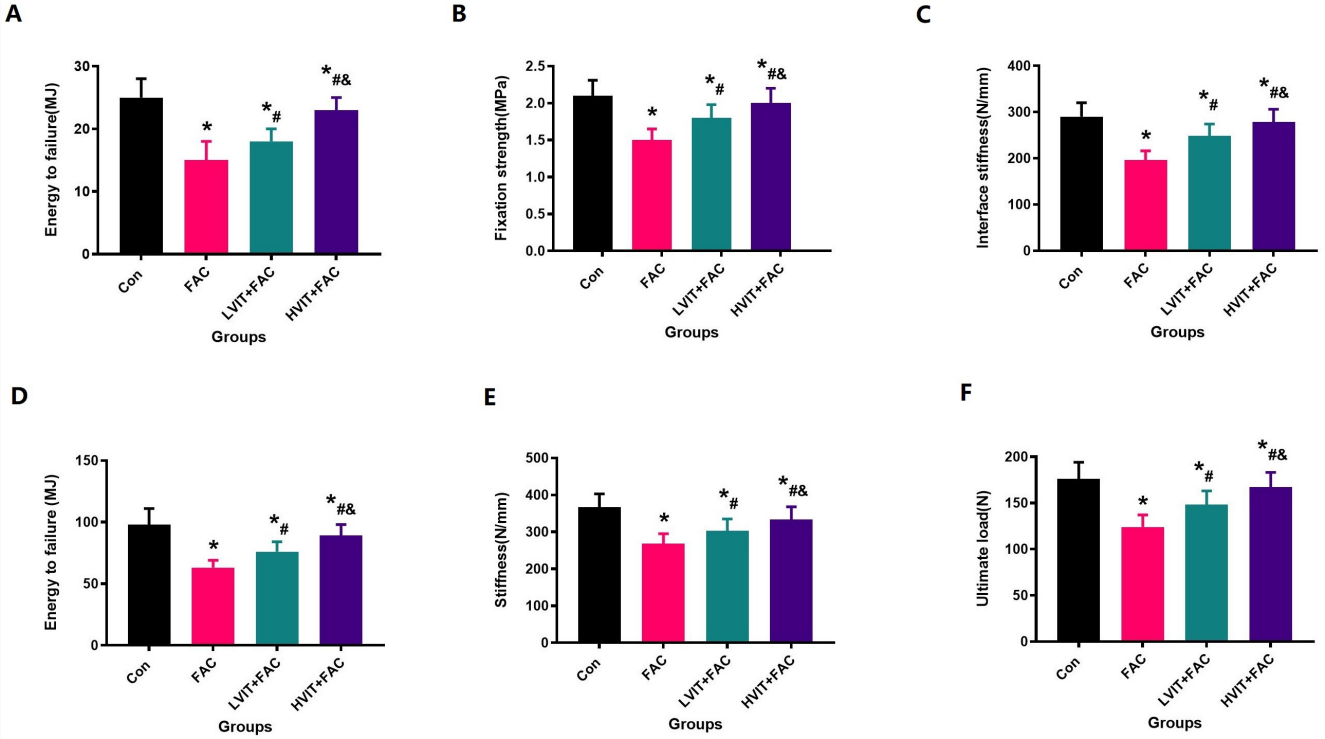

Fig. 4

Vericiguat (VIT) treatment significantly enhanced titanium rod stability and femoral bone strength through pull-out test including a) energy to failure, b) fixation strength, and c) interface stiffness, and three-point bending test including d) energy to failure, e) stiffness, and f) ultimate load in different experimental groups (Con, ferric ammonium citrate (FAC), lower VIT (LVIT) + FAC, higher VIT (HVIT) + FAC). There were five specimens per group. * = vs Control group, p = 0.012; # = vs FAC, p = 0.023; & = vs LVIT + FAC group, p = 0.019. All independent-samples *t*-test and one-way analysis of variance.

cross-linked telopeptide of type 1 collagen (CTX), serum cytokines including tumour necrosis factor-alpha (TNF-α), interleukin-1β (IL-1β), and interleukin-6 (IL-6), were analyzed using a commercially available ELISA kit from My BioSource (USA). The levels of malondialdehyde (MDA), nitric oxide (NO), superoxide dismutase (SOD), and reduced glutathione (GSH) were detected in the serum by using the assay kits from Nanjing Jiancheng Biotechnology (China).

MC3T3-E1 cell and RAW264.7 cell experiments

In this study, murine osteoblast cell line MC3T3-E1 was used for the in vitro tests, which was purchased from Shanghai Cell Bank. Dulbecco's Modified Eagle's Medium (DMEM) was used for the cell culture media. Mouse macrophage RAW264.7 cells acquired from Shanghai Bangjing Industrial (China) were used to test the inductive effect of FAC and VIT on osteoclastogenesis. Initially, MC3T3-E1 cells and RAW264.7 cells (1×10^4 cells/ml) were cultured under different conditions as follows: 1) normal medium (Con); 2) FAC treatment group (10 mM; Sigma); 3) FAC + VIT treatment (FAC + VIT); and 4) FAC + deferoxamine (an iron chelating agent, DPO, 10 mM; Sigma) treatment (FAC + DPO). Dosages used for FAC and DPO in MC3T3-E1 cell experiments were chosen according to a previous study.[32,33]

Cell proliferation assay, alkaline phosphatase staining, and alizarin red staining

A Cell-Counting Kit-8 (CCK-8; Dojindo Laboratories, Japan) was used to determine cell proliferation according to previous reports.[34,35] Briefly, MC3T3-E1 cells were cultured in 24-well plates at a density of 5×10^4 cells per well, and then incubated with DPO, FAC, and different concentrations of VIT. The effects of different interference factors on cell proliferation activity at different times (6 hrs, 12 hrs, 24 hrs) were detected by the CCK-8 kit. Next, CCK-8 solution was added to the culture medium and cultured for an additional four hours at 37°C. The absorbance values were then observed using a 450 nm wavelength microplate reader (BioTek, USA). Afterwards, osteogenic differentiation of the MC3T3-E1 was induced using osteogenic differentiation medium, containing 0.15 mM ascorbate-2-phosphate, 2 mM β-glycerophosphate, and 10 mM dexamethasone (Sigma-Aldrich). MC3T3-E1 was seeded onto six-well plates with 1×10^5 cells per well. When MC3T3-E1 reached confluence, osteogenic differentiation media were added and co-cultured for 14 or 21 days. The osteogenic differentiation medium and FAC, VIT, and DPO were exchanged every 48 hours. Following this, the treated cells were subjected to alkaline phosphatase (ALP) or alizarin red (ARS) staining (Rainbow Biotechnology, China) according to the manufacturers' protocols. For ALP staining, following the differentiation period for 14 days, the cells were firstly washed with phosphate-buffered saline (PBS) three times, fixed with 4% paraformaldehyde for 15 minutes, and then washed again but with double-distilled water (ddH_2O) every three minutes, three times. Finally, the cells were stained with the BCIP/NBT ALP color development kit (Beyotime Biotechnology, China). For ARS staining, following the differentiation period for 21 days, the cells were fixed in 4% paraformaldehyde and treated with 40 mM ARS solution at room temperature for 30 minutes. Quantitative analysis

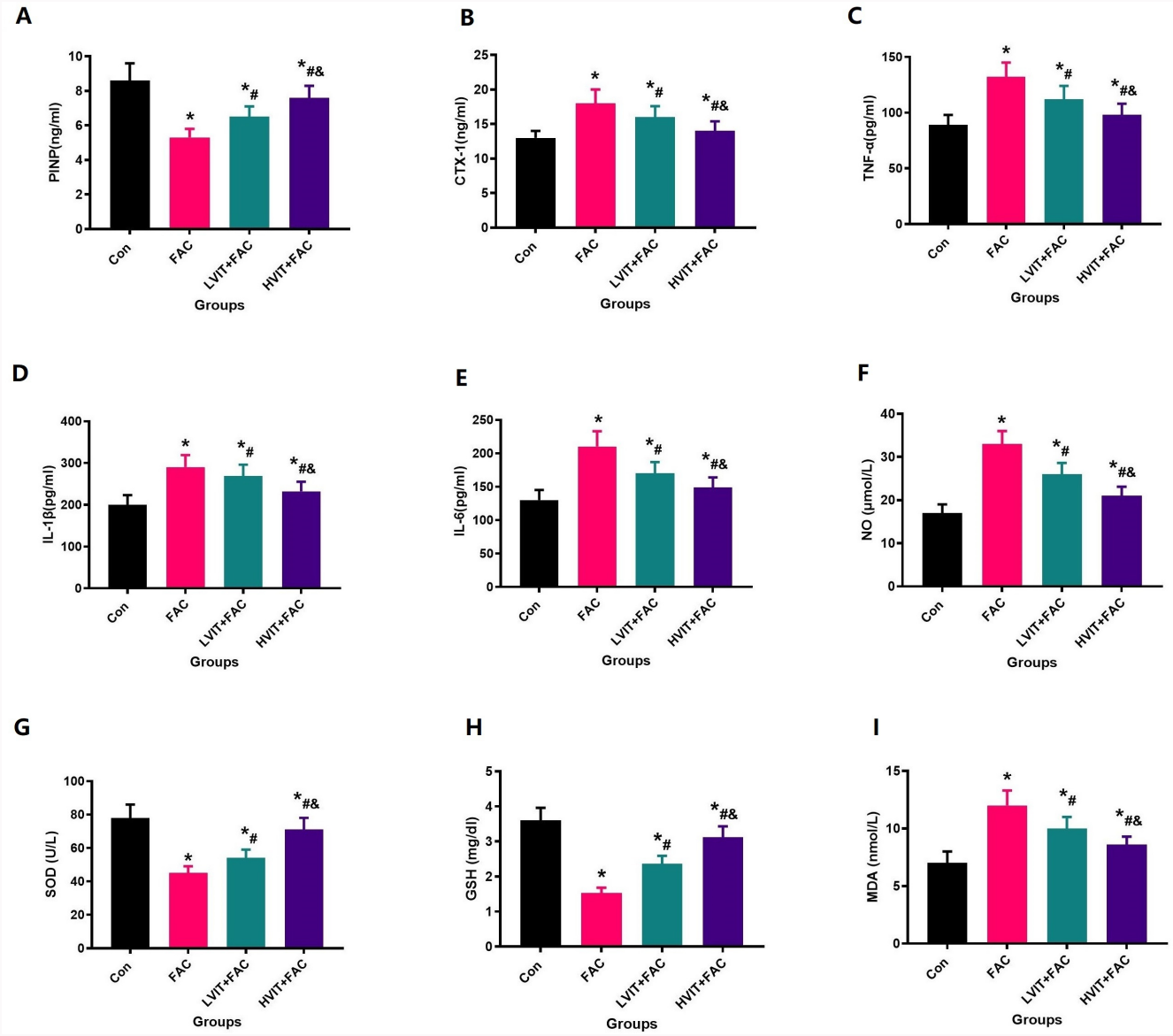

Fig. 5

The alterations in bone metabolism markers, inflammatory factors, and oxidative stress indicators were assessed following the intervention in each group, including a) procollagen type 1 N-terminal propeptide (P1NP), b) C-terminal telopeptide (CTX), c) TNF-α, d) IL-1β, e) IL-6, f) NO, g) SOD, h) GSH, and i) MDA. There were five specimens per group. * = vs Control group, p = 0.017; # = vs FAC, p = 0.034; & = vs LVIT + FAC group, p = 0.042. All independent-samples *t*-test and one-way analysis of variance.

was performed by adding a 5% perchloric acid solution to each well and measuring the absorbance at a wavelength of 420 nm using a spectrophotometer (BioTek).

After 48 hours of intervention with FAC, VIT, and DPO, the changes in reactive oxygen species (ROS) levels of MC3T3-E1 cells and mitochondria following the intervention were evaluated using 2',7'-dichlorofluorescein diacetate (DCFH-DA, Sigma-Aldrich) staining and MitoSOX Red mitochondrial superoxide indicator (MitoSOX, Sigma-Aldrich) staining. To measure the levels of intracellular ROS, MC3T3-E1 were incubated with 10 μM DCFH-DA for 30 minutes at 37°C. To measure the levels of mitochondrial superoxides, MC3T3-E1 were incubated with 5 μM Mito SOXTM Red Mitochondrial Superoxide Indicator for ten minutes at 37°C. After washing with PBS, the cells were observed using an Olympus IX51 microscope (Olympus, Japan).

The lipophilic cationic probe 5,5',6,6'-tetrachloro-1,1',3,3'-tetraethyl-imida-carbocyanine iodide (JC-1) was applied to detect the mitochondrial membrane potential. After experimentation, 2 μM JC-1 (Beyotime Biotechnology, S0033 M) was added to the cells, and the cells were incubated for 30 minutes at 37°C in the dark. After washing the cells three times with PBS, the nuclei were stained with Hochest 33,258. The results were observed by fluorescence microscope. The levels of malondialdehyde (MDA) and total SOD activity in the cells were measured by a malondialdehyde detection assay kit (APPLYGEN, China) and SOD activity assay kit (Abcam, UK), respectively.

In order to further intuitively explore whether VIT can resist the effect of FAC on osteoclast differentiation, the differentiation of RAW264.7 cells in the osteoclast direction was induced by 100 ng/ml RANKL for four days as described previously.[36] Then, FAC and/or VIT was added to the medium

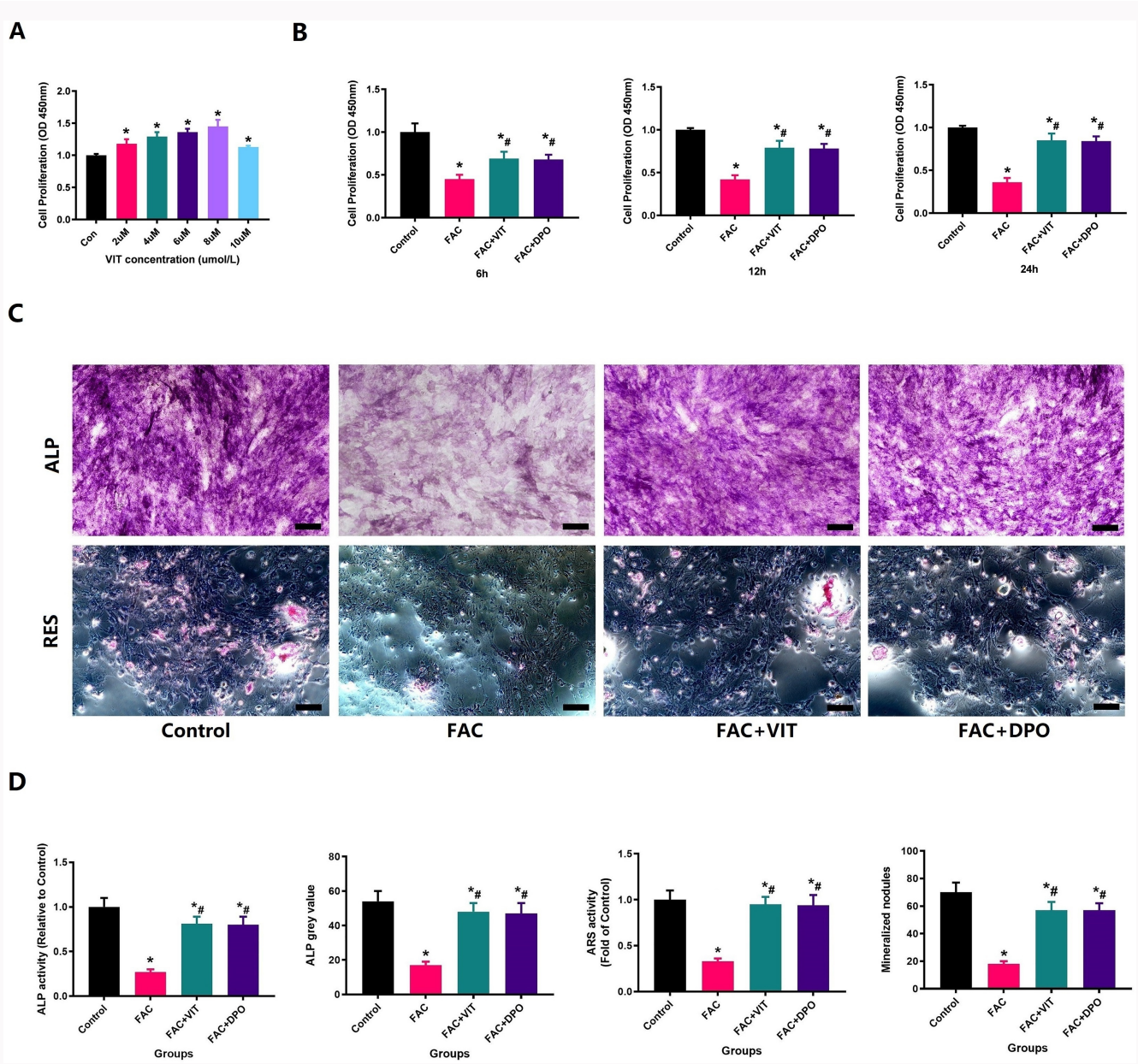

Fig. 6

The impact of vericiguat (VIT) on the growth rate and osteogenic differentiation of MC3T3-E1 cells treated with ferric ammonium citrate (FAC). a) Cell Counting Kit (CCK)-8 assay was employed to assess cell proliferation at various concentrations of VIT for 24 hours. b) CCK-8 assay was conducted to evaluate the effect of VIT on cell proliferation rate at a concentration of 8 μM for durations of six, 12, and 24 hours. c) Representative images of high-magnification alkaline phosphatase (ALP) and alizarin red (RES) staining are depicted to evaluate osteogenic differentiation. Scale bar: 50 μm, magnification ×40. d) Quantitative results obtained from ALP staining and Alizarin red staining include measurements of ALP activity levels, grey values of ALP, mineralized areas, and mineralized nodules. There were five specimens per group. * = vs Control group, p = 0.016; # = vs FAC, p = 0.005; & = vs FAC + VIT group, p = 0.028. All independent-samples *t*-test and one-way analysis of variance.

and the cells were placed under standard culture conditions for seven days. Subsequently, TRAP staining kit (Sigma-Aldrich) was used to stain and evaluate the cells after intervention to determine the osteoclastic differentiation of RAW264.7.

Statistical analysis

The mean and SD values for each group, consisting of n = 5/group, were reported and statistical analysis was performed using SPSS 19.0 for Windows (IBM, USA). Normality of the variables was checked using the Kolmogorov-Smirnov test. The independent-samples *t*-test and one-way analysis of variance (ANOVA) were used to test differences among different groups. A significance level of $p < 0.05$ was considered statistically significant.

Results

In order to investigate the effects of VIT on the integration of titanium rods in the distal femur of rats treated with FAC, we used micro-CT and Von Gieson techniques to analyze changes in bone mineral density (BMD) and surrounding bone tissue near the titanium rod. Our results showed that osseointegration of titanium rods was significantly hindered in rats treated with FAC, as evidenced by less bone formation around the titanium rods (Figure 1). Furthermore, our micro-CT evaluation revealed that rats treated with VIT had higher BMD, BV/TV, Tb.

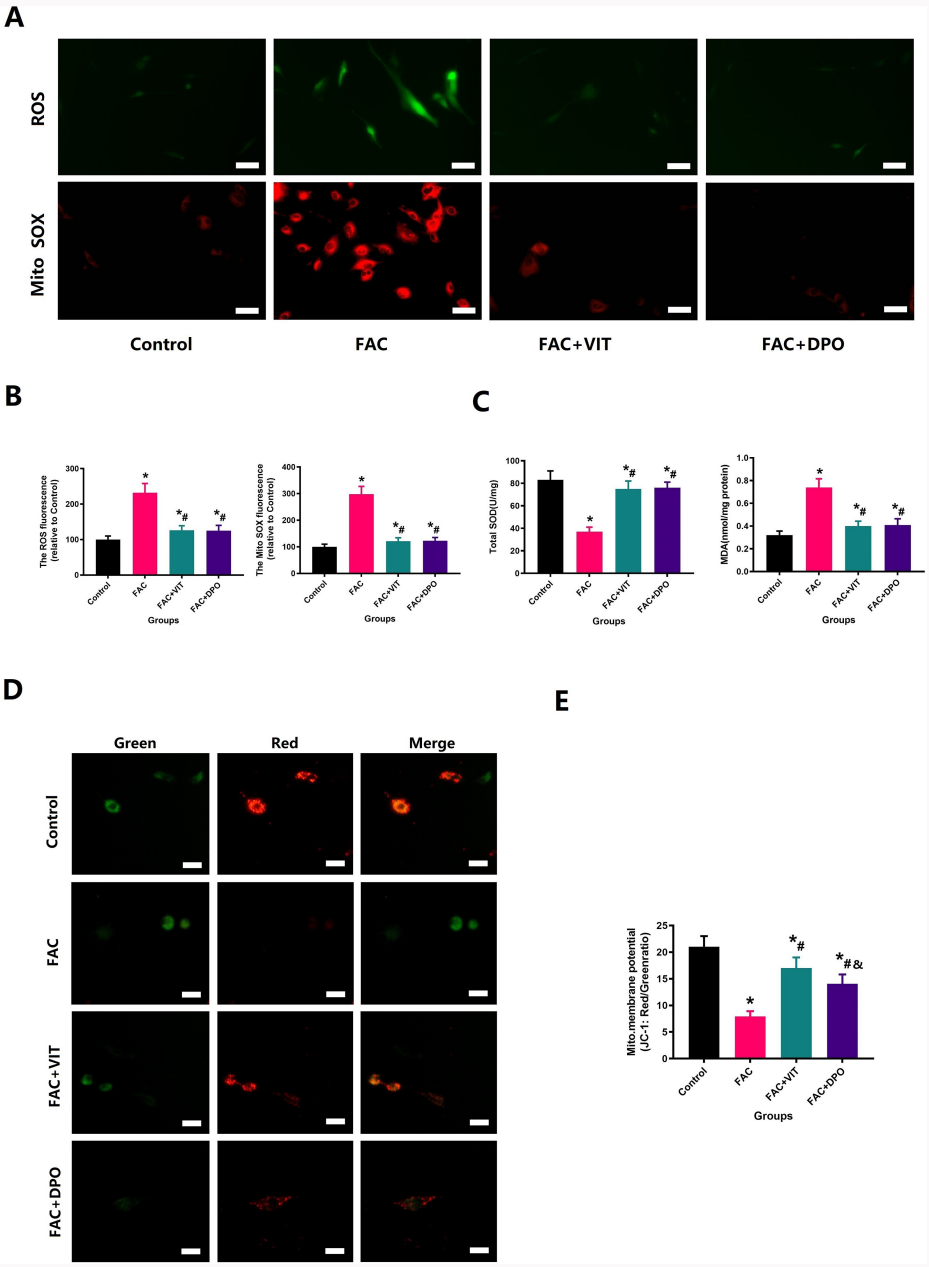

Fig. 7

Vericiguat (VIT) significantly reduced oxidative stress and protected mitochondrial membrane potential in ferric ammonium citrate (FAC)-treated cells. a) Representative images of MC3T3-E1 cells subjected to different intervention conditions, demonstrating the levels of intracellular Mito SOX and reactive oxygen species (ROS). The scale bar corresponds to a length of 25 μm. b) The quantitative results for intracellular Mito SOX and ROS in MC3T3-E1 cells. c) The SOD and MDA levels of MC3T3-E1 cells in different groups; n = 5/group. d) Representative images of MC3T3-E1 cells subjected to different intervention conditions, demonstrating the changes in mitochondrial model potential. The scale bar corresponds to a length of 25 μm. e) Quantitative results for JC-1 in MC3T3-E1 cells. There were five specimens per group. * = vs Control group, p = 0.006; # = vs FAC, p = 0.019; & = vs FAC + VIT group, p = 0.037. All independent-samples *t*-test and one-way analysis of variance.

Th, and Tb. N, and lower Tb. Sp, compared to those in the FAC group ($p < 0.01$, independent-samples *t*-test and one-way ANOVA; Figure 1b). Additionally, histomorphometric analysis demonstrated that systemic administration of VIT significantly increased bone area ratio (BAR) and bone-to-implant contact (BIC) compared to the FAC group ($p < 0.01$; Figures 1c and 1d). These findings suggest that iron overload may negatively impact new bone formation on titanium implants, but treatment with VIT can mitigate these adverse effects on osseointegration.

The BMD and BMC of the distal femur in the FAC rats exhibited a statistically significant decrease compared to those in the Con group (Figure 2). Micro-CT analysis was conducted to evaluate the trabecular bone microstructure of the distal femur. The results from micro-CT assessment indicated that BV/TV, Tb. Th, Tb. N were reduced, while Tb. Sp was increased in the FAC rats when compared to the VIT-treated groups (Figure 2). To further explore pathological alterations in trabecular bone microstructure, decalcified femora from each group underwent HE and Masson staining procedures. Staining with HE and Masson revealed a decline in cancellous

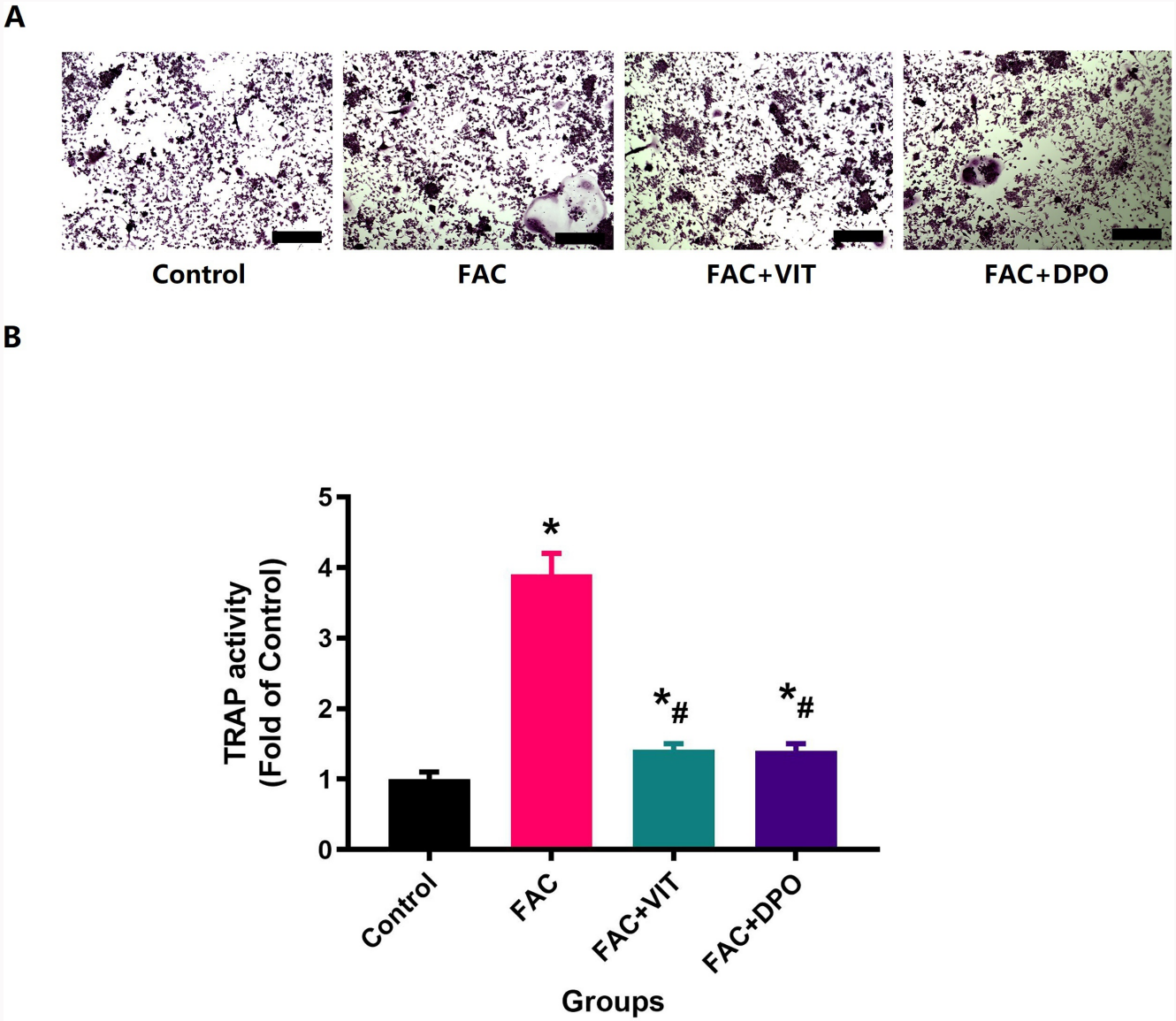

Fig. 8

The decrease in tartrate-resistant alkaline phosphatase (TRAP)-positive areas was quantified and demonstrated that vericiguat (VIT) significantly reduced ferric ammonium citrate (FAC)-induced osteoclast activity. a) Upon the addition of VIT, there was a significant reduction in the elevated expression levels of TRAP caused by iron overload (scale bar = 50 μm, magnification ×20). b) This decrease in TRAP staining-positive areas allowed for quantitative analysis. There were five specimens per group. * = vs Control group, p = 0.004; # = vs FAC, p = 0.035; & = vs FAC + VIT group, p = 0.023. All independent-samples *t*-test and one-way analysis of variance.

bone density, decreased volume of trabecular bone, and diminished presence of bone marrow in the FAC group; however, these deficiencies showed statistically significant improvement with VIT treatment (Figure 2).

In order to investigate the impact of osteoblast and osteoclast activity on bone reconstruction, we used immunohistochemical detection methods to observe the expression levels of OC and TRAP in rat bone (Figure 3a). As expected, the presence of FAC was found to suppress OC expression while promoting TRAP generation (Figure 3b). Conversely, treatment with VIT resulted in an increase in OC expression and a decrease in TRAP expression in the bone tissue (Figure 3b). These findings suggest that VIT may have a protective effect against bone loss, and enhance osseointegration ability in aged rats treated with FAC by stimulating osteoblast activity and inhibiting osteoclast function.

In order to investigate the impact of VIT treatment on femoral bone strength and titanium rod stability in different groups, biomechanical tests were conducted. The experimental results directly indicated a significant decrease in the stability of the titanium implant in the femur 12 weeks after implantation due to FAC treatment, along with a reduction in femoral bone strength (Figure 4; $p < 0.05$, independent-samples *t*-test and one-way ANOVA). However, it was observed that VIT treatment considerably improved osseointegration of the titanium rod and enhanced bone strength in aged rats with iron overload (Figure 4; $p < 0.05$, independent-samples *t*-test and one-way ANOVA). Biomechanical parameters suggest that administration of VIT could enhance both the stability of titanium implants and bone strength in FAC-treated aged rats.

To assess the effects of FAC and VIT on osteoblasts and osteoclasts in aged rats, we conducted a study measuring serum levels of procollagen type 1 N-terminal propeptide (P1NP) and C-terminal telopeptide (CTX-1) as indicators of bone turnover. Our results indicated a significant reduction in serum P1NP levels, while rats treated with VIT exhibited higher CTX-1 levels compared to those in the FAC group ($p < 0.05$) (Figure 5). Excessive buildup of iron leads to programmed cell death, and impedes function by triggering oxidative stress and inflammation.[37] Hence, in our investigation, we employed serum marker levels such as TNF-α, IL-1β, IL-6, MDA, NO, SOD, and GSH to serve as indicators for assessing the extent of oxidative stress and inflammation in rats. Compared to the FAC group, the VIT treatment group displayed a significant decrease in levels of TNF-α, IL-1β, IL-6, MDA, and NO while showing increased levels of SOD and GSH ($p < 0.05$). These compelling findings strongly indicate that VIT treatment effectively mitigated oxidative stress and inflammation induced by FAC in aged rats.

To assess the influence of varying levels of VIT on cell proliferation rate in the presence of FAC treatment, cells were exposed to different concentrations of VIT (2 μM, 4 μM, 6 μM, 8 μM, 10 μM) for a duration of 24 hours in this experimental investigation. Subsequently, the CCK-8 assay was used to determine the rate at which cells proliferated. As depicted in Figure 6a, there is a downward trend of the relationship between VIT concentration and cell proliferation rate when comparing concentrations ranging from 8 to 10 μM. We also explored the impact of different time periods (6 hrs, 12 hrs, and 24 hrs) with a constant concentration of VIT at 8 μM on MC3T3-E1 proliferation rate as illustrated in Figure 6b. The present study revealed that VIT exerted a protective effect against the inhibition of MC3T3-E1 proliferation induced by FAC treatment.

Based on the findings from ALP and ARS staining (Figure 6c), as well as Mito SOX staining for cellular and mitochondrial ROS (Figure 7a) and measurement of mitochondrial membrane potential (Figure 7d), it was observed that treatment with 8 μM of VIT significantly enhanced the expression of ALP in FAC-treated MC3T3-E1 cells, leading to improved mineralization and increased formation of calcium nodules ($p < 0.05$, independent-samples *t*-test and one-way ANOVA, Figure 6d). Moreover, VIT treatment resulted in a significant reduction in ROS and Mito SOX production in MC3T3-E1 cells ($p < 0.05$, independent-samples *t*-test and one-way ANOVA, Figure 7b). Additionally, VIT exhibited the ability to partially restore changes in mitochondrial membrane potential caused by FAC intervention ($p < 0.05$, independent-samples *t*-test and one-way ANOVA, Figure 7e). Furthermore, DPO intervention effectively mitigated the adverse effects induced by FAC. The results obtained from staining techniques and quantitative analysis demonstrated that VIT exerted a protective effect on the osteogenic capacity of MC3T3-E1 cells by reducing oxidative stress levels induced by FAC exposure.

According to the results obtained from TRAP staining (Figure 8a) and quantitative evaluation (Figure 8b), it was observed that the presence of TRAP in RAW264.7 cells treated with FAC exhibited a significant reduction following exposure to 8 μm of VIT ($p < 0.05$). The results of both staining and quantitative analysis indicated an adverse impact of VIT on the osteoclastogenesis ability of FAC-treated RAW264.7 cells, suggesting its potential inhibitory role in this process.

Discussion

In recent years, the failure rates of implants, one of the most feared but often encountered complications in the practice of an orthopaedic surgeon, have rapidly increased, especially in osteoporosis patients.[38,39] The main reason for the failure of the orthopaedic implant is bone loss around the implants, which is caused by a series of risk factors.[40,41] Despite advances in surgical techniques and pharmacology, the treatment of osteoporotic fractures remains challenging.[42] Abnormal bone remodelling due to age leads to periprosthetic bone loss, and aggravates orthopaedic implant loosening.[39,43] Therefore, removing the influence of bone loss is a key way to reduce implant failure rates, and requires particular attention for further treatment.

Increasing evidence has confirmed that abnormal iron metabolism, especially iron overload, may adversely affect osteoblasts and therefore bone mass.[15] Research has also shown a close association between iron metabolism and bone metabolism,[15] with iron playing a critical role in maintaining bone mass homeostasis.[44] Excessive iron can disrupt the delicate balance between bone resorption and formation, potentially leading to osteopenia and even osteoporosis.[16] As iron overload causes undesirable side effects and has a negative impact on bone mass, we hypothesized that iron overload has negative side effects on osseointegration of orthopaedic implants. In this study, 24-month-old male SD rats were used as experimental animals because the skeletal metabolic status of rats at this age is similar to that experienced by older males.[45,46] At the same time, five older rats and five younger rats were selected and killed to obtain the femora for histological and micro-CT evaluation. Our results confirmed that iron overload under experimental conditions has harmful effects on osseointegration in an aged rat model.

This study only preliminarily explored how guanylate cyclase promotes osseointegration under iron overload, which may be related to inhibiting oxidative stress and inflammation; the exact mechanism remains unclear. An additional limitation is that we did not use melatonin as a positive control, so further verification is needed.

Successful osseointegration of orthopaedic implants relies on new bone forming around the implant surface and connecting to the implant site.[47] The peri-implant bone needs to undergo a continuous remodelling process after the implant is placed with appropriate bone tissue.[48] In the case of successful osseointegration, the first requirement is that the implant site requires sufficient bone mass for the implant to achieve primary stability.[49] In order to achieve subsequent successful osseointegration of implants and keep them functioning effectively in the long term, it is necessary to achieve secondary stability, i.e. bone formation and remodelling around implants, and fusion with recipient bone.[50] In this study, we showed that iron overload decreased the generation of new bone around titanium rods and promoted bone turnover, which is consistent with previous results.[32] In other rat models, the harmful effects of FAC on the microstructure of bone trabeculae on the distal femur of osteoporosis rats was confirmed by several outcome measures, including decreased

BV/TV, Tb. N, BMD, and Tb. Th, and increased osteoblast and osteoclast activity and Tb. Sp.[32] We found that treatment with VIT for 12 weeks in FAC-treated rats resulted in a significant enhancement of osseointegration at the femoral epiphysis. These findings suggest that the negative effects were most likely due to the effect of iron overload on increased ROS production and inflammation, and that the ability of VIT to reverse this effect may be related to a reduction in oxidative stress and inflammation,[51] which is supported by a previous study showing a reduction in bone mass when treated with FAC.[52]

So far, although there has not yet been a report about the direct relationship between iron overload and osseointegration in orthopaedics, bone loss due to iron overload might be a result of stimulation of osteoclastogenesis or inhibition of osteoblast functions through stimulation of ROS and inflammatory cytokine production.[53] The markers P1NP and CTX, widely used and highly sensitive indicators of bone metabolism, are capable of accurately reflecting the current state of bone metabolism.[24,25] Reduced P1NP levels and increased CTX production were observed in the FAC treatment group, suggesting enhanced bone resorption and impaired bone formation. Mitochondrial membrane potential refers to the voltage difference across the inner and outer membranes of mitochondria.[54] Changes in the mitochondrial membrane potential can influence the activity of ion channels, transporters, and enzymes, leading to alterations in cell function and behaviour.[54] The JC-1 staining method provides an accurate reflection of changes in mitochondrial membrane potential, thereby indicating the cellular state of mitochondrial function. As iron overload-induced cell and organ damage is associated with excessive ROS and inflammatory cytokine production, we further examined the changes of serum oxidative stress and inflammation specific markers in this study. MDA and SOD are two specific and representative markers that quantify changes in oxidative stress that are closely linked to osteoporosis.[55] Additionally, TNF-α, IL-6, and IL-1β are the most classical markers of pro-inflammatory cytokines and can be used to directly reflect the level of inflammation.[56] Therefore, changes in SOD, MDA, TNF-α, IL-6, and IL-1β levels may indicate production of ROS and inflammation caused by FAC. It is known that osteoblasts serve an important role in bone regeneration in physiological conditions and also coordinate the activities of osteoclasts.[57] Therefore, in order to more intuitively explore the effect of FAC on the proliferation, differentiation, and activity of osteoblasts and osteoclasts, in vitro experiments were performed. Based on our cell experiments, we observed that the dose of FAC used in the experiments showed negative effects on osteogenic differentiation, such as inhibition of proliferation and suppression of differentiation of osteoblasts. Furthermore, it can increase osteoclast activity by inducing RAW264.7 cell differentiation to osteoclasts. These data indicate that iron overload can increase the level of oxidative stress and inflammation in male SD rats, thus inhibiting the proliferation and differentiation of osteoblasts and reducing their activity, while promoting the formation of osteoclasts, thereby leading to a reduction of osseointegration in aged rats. Therefore, we believe that VIT holds significant clinical potential in the prevention and treatment of osteoporotic fractures in elderly individuals, as well as in reducing joint prosthesis loosening, particularly among those with potential iron overload. VIT is a recently approved drug in the clinical setting, offering a notable advantage of safety and minimal side effects.

Taken together, the results from our experiments confirmed that VIT can stimulate proliferation and osteogenic differentiation, and inhibit osteoclast differentiation by inhibition of oxidative stress and inflammation, leading to improvement of bone regeneration around titanium rods in aged rats with FAC treatment. However, no further mechanistic signalling pathway studies or drug dose experiments have been performed, so subsequent studies will focus on these shortcomings.

Supplementary material

Outline of animal population requirements, and ARRIVE checklist.

References

1. **Garg G**, **Kumar J**, **McGuigan FE**, **et al**. Variation in the MC4R gene is associated with bone phenotypes in elderly Swedish women. *PLoS One*. 2014;9(2):e88565.
2. **Xu W**, **Ganz C**, **Weber U**, **et al**. Evaluation of injectable silica-embedded nanohydroxyapatite bone substitute in a rat tibia defect model. *Int J Nanomedicine*. 2011;6:1543–1552.
3. **Abe S**, **Kashii M**, **Shimada T**, **et al**. Relationship between distal radius fracture severity and 25-hydroxyvitamin-D level among perimenopausal and postmenopausal women. *Bone Jt Open*. 2022;3(3):261–267.
4. **Brech GC**, **Bobbio TG**, **Cabral KN**, **et al**. Changes in postural balance associated with a woman's aging process. *Clinics (Sao Paulo)*. 2022; 77:100041.
5. **Li H**, **Duan X**, **Wu Z**, **Qin Y**. Feasibility of laparoscopic enucleation for hemangioma in special hepatic segments. *Front Surg*. 2022;9:1111307.
6. **Williamson TK**, **Passfall L**, **Ihejirika-Lomedico R**, **et al**. Assessing the influence of modifiable patient-related factors on complication rates after adult spinal deformity surgery. *Bone Joint J*. 2022;104-B(11):1249–1255.
7. **Joshi A**, **Dias G**, **Staiger MP**. *In silico* modelling of the corrosion of biodegradable magnesium-based biomaterials: modelling approaches, validation and future perspectives. *Biomater Transl*. 2021;2(3):257–271.
8. **Knudsen MB**, **Thillemann JK**, **Jørgensen PB**, **Jakobsen SS**, **Daugaard H**, **Søballe K**. Electrochemically applied hydroxyapatite on the cementless porous surface of bi-metric stems reduces early migration and has a lasting effect: an efficacy trial of a randomized five-year follow-up radiostereometric study. *Bone Joint J*. 2022;104-b(6):647–656.
9. **Choi NH**, **Yoon HI**, **Kim TH**, **Park EJ**. Improvement in fatigue behavior of dental implant fixtures by changing internal connection design: an in vitro pilot study. *Materials (Basel)*. 2019;12(19):19.
10. **Bukowski BR**, **Sandhu KP**, **Bernatz JT**, **et al**. CT required to perform robotic-assisted total hip arthroplasty can identify previously undiagnosed osteoporosis and guide femoral fixation strategy. *Bone Joint J*. 2023;105-B(3):254–260.
11. **Ha J-H**, **Doguer C**, **Wang X**, **Flores SR**, **Collins JF**. High-iron consumption impairs growth and causes copper-deficiency anemia in weanling Sprague-Dawley rats. *PLoS One*. 2016;11(8):e0161033.
12. **Miao R**, **Fang X**, **Zhang Y**, **Wei J**, **Zhang Y**, **Tian J**. Iron metabolism and ferroptosis in type 2 diabetes mellitus and complications: mechanisms and therapeutic opportunities. *Cell Death Dis*. 2023;14(3):186.
13. **Mahalhal A**, **Burkitt MD**, **Duckworth CA**, **et al**. Long-term iron deficiency and dietary iron excess exacerbate acute dextran sodium sulphate-induced colitis and are associated with significant dysbiosis. *Int J Mol Sci*. 2021;22(7):3646.
14. **Hänninen MM**, **Haapasalo J**, **Haapasalo H**, **et al**. Expression of iron-related genes in human brain and brain tumors. *BMC Neurosci*. 2009; 10:36.
15. **Zhao G-Y**, **Dl D-H**, **Wang B**, **Zhang P**, **Xu Y-J**. Iron regulates the expression of ferroportin 1 in the cultured hFOB 1.19 osteoblast cell line. *Exp Ther Med*. 2014;8(3):826–830.

16. **Li GF**, **Pan YZ**, **Sirois P**, **Li K**, **Xu YJ**. Iron homeostasis in osteoporosis and its clinical implications. *Osteoporos Int*. 2012;23(10):2403–2408.
17. **Sun K**, **Kong F**, **Lin F**, **et al**. Vericiguat modulates osteoclast differentiation and bone resorption via a balance between VASP and NF-κB pathways. *Mediators Inflamm*. 2022;2022:1625290.
18. **Rangaswami H**, **Schwappacher R**, **Marathe N**, **et al**. Cyclic GMP and protein kinase G control a Src-containing mechanosome in osteoblasts. *Sci Signal*. 2010;3(153):ra91.
19. **US Food & Drug Administration**. 2021. https://www.accessdata.fda.gov/drugsatfda_docs/appletter/2021/214377Orig1s000ltr.pdf (date last accessed 1 August 2024).
20. **Kaplinsky E**, **Perrone S**, **Barbagelata A**. Emerging concepts in heart failure management and treatment: focus on vericiguat. *Drugs Context*. 2023;12:12.
21. **Gheorghiade M**, **Greene SJ**, **Butler J**, **et al**. Effect of vericiguat, a soluble guanylate cyclase stimulator, on natriuretic peptide levels in patients with worsening chronic heart failure and REDUCED ejection fraction: the SOCRATES-REDUCED randomized trial. *JAMA*. 2015;314(21):2251–2262.
22. **Hoareau GL**, **Williams TK**, **Davidson AJ**, **et al**. Endocrine effects of simulated complete and partial aortic occlusion in a swine model of hemorrhagic shock. *Mil Med*. 2019;184(5–6):e298–e302.
23. **Biswas K**, **Couillard M**, **Cavallone L**, **et al**. A novel mouse model of PMS2 founder mutation that causes mismatch repair defect due to aberrant splicing. *Cell Death Dis*. 2021;12(9):838.
24. **Zhou MS**, **Tao ZS**. Systemic administration with melatonin in the daytime has a better effect on promoting osseointegration of titanium rods in ovariectomized rats. *Bone Joint Res*. 2022;11(11):751–762.
25. **Tao ZS**, **Li TL**, **Xu HG**, **Yang M**. Hydrogel contained valproic acid accelerates bone-defect repair via activating Notch signaling pathway in ovariectomized rats. *J Mater Sci Mater Med*. 2021;33(1):4.
26. **Li YF**, **Li XD**, **Bao CY**, **Chen QM**, **Zhang H**, **Hu J**. Promotion of peri-implant bone healing by systemically administered parathyroid hormone (1-34) and zoledronic acid adsorbed onto the implant surface. *Osteoporos Int*. 2013;24(3):1063–1071.
27. **Gabet Y**, **Kohavi D**, **Kohler T**, **Baras M**, **Müller R**, **Bab I**. Trabecular bone gradient in rat long bone metaphyses: mathematical modeling and application to morphometric measurements and correction of implant positioning. *J Bone Miner Res*. 2008;23(1):48–57.
28. **Tao Z-S**, **Wu X-J**, **Zhou W-S**, **et al**. Local administration of aspirin with β-tricalcium phosphate/poly-lactic-co-glycolic acid (β-TCP/PLGA) could enhance osteoporotic bone regeneration. *J Bone Miner Metab*. 2019;37(6):1026–1035.
29. **Tao Z**, **Zhou W**, **Wu X**, **et al**. Local administration of aspirin improves osseointegration of hydroxyapatite-coated titanium implants in ovariectomized rats through activation of the Notch signaling pathway. *J Biomater Appl*. 2020;34(7):1009–1018.
30. **Li Y**, **Li Q**, **Zhu S**, **et al**. The effect of strontium-substituted hydroxyapatite coating on implant fixation in ovariectomized rats. *Biomaterials*. 2010;31(34):9006–9014.
31. **Tao Z-S**, **Wu X-J**, **Yang M**, **Xu H-G**. Local administration with silymarin could increase osseointegration of hydroxyapatite-coated titanium implants in ovariectomized rats. *J Biomater Appl*. 2019;34(5):664–672.
32. **Tao ZS**, **Li TL**, **Wei S**. Silymarin prevents iron overload induced bone loss by inhibiting oxidative stress in an ovariectomized animal model. *Chem Biol Interact*. 2022;366:110168.
33. **Wang W**, **Jing X**, **Du T**, **et al**. Iron overload promotes intervertebral disc degeneration via inducing oxidative stress and ferroptosis in endplate chondrocytes. *Free Radic Biol Med*. 2022;190:234–246.
34. **Tao ZS**, **Zhou WS**, **Xu HG**, **Yang M**. Simvastatin can enhance the osseointegration of titanium rods in ovariectomized rats maintenance treatment with valproic acid. *Biomed Pharmacother*. 2020;132:110745.
35. **Tao ZS**, **Zhou WS**, **Xu HG**, **Yang M**. Aspirin modified strontium-doped β-tricalcium phosphate can accelerate the healing of femoral metaphyseal defects in ovariectomized rats. *Biomed Pharmacother*. 2020;132:110911.
36. **Tang D**, **Liu X**, **Chen K**, **et al**. Cytoplasmic PCNA is located in the actin belt and involved in osteoclast differentiation. *Aging (Albany NY)*. 2020;12(13):13297–13317.
37. **Vannocci T**, **Dinarelli S**, **Girasole M**, **Pastore A**, **Longo G**. A new tool to determine the cellular metabolic landscape: nanotechnology to the study of Friedreich's ataxia. *Sci Rep*. 2019;9(1):19282.
38. **Zhou W**, **Liu Y**, **Shen J**, **et al**. Melatonin increases bone mass around the prostheses of OVX rats by ameliorating mitochondrial oxidative stress via the SIRT3/SOD2 signaling pathway. *Oxid Med Cell Longev*. 2019;2019:4019619.
39. **Staats K**, **Sosa BR**, **Kuyl E-V**, **et al**. Intermittent parathyroid hormone increases stability and improves osseointegration of initially unstable implants. *Bone Joint Res*. 2022;11(5):260–269.
40. **Jin J**, **Zhang L**, **Shi M**, **Zhang Y**, **Wang Q**. Ti-GO-Ag nanocomposite: the effect of content level on the antimicrobial activity and cytotoxicity. *Int J Nanomedicine*. 2017;12:4209–4224.
41. **Thomas J**, **Shichman I**, **Ohanisian L**, **et al**. Monoblock tapered stems in management of UCS B2 and B3 periprosthetic fractures in revision total hip arthroplasty. *Bone Jt Open*. 2023;4(8):551–558.
42. **Talic A**, **Kapetanovic J**, **Dizdar A**. Effects of conservative treatment for osteoporotic thoracolumbal spine fractures. *Mater Sociomed*. 2012;24(1):16–20.
43. **Hijikata Y**, **Kamitani T**, **Nakahara M**, **et al**. Development and internal validation of a clinical prediction model for acute adjacent vertebral fracture after vertebral augmentation: the AVA score. *Bone Joint J*. 2022;104-B(1):97–102.
44. **Guo JP**, **Pan JX**, **Xiong L**, **Xia WF**, **Cui S**, **Xiong WC**. Iron chelation inhibits osteoclastic differentiation in vitro and in Tg2576 mouse model of Alzheimer's disease. *PLoS One*. 2015;10(11):e0139395.
45. **Luo D**, **Ren H**, **Li T**, **Lian K**, **Lin D**. Rapamycin reduces severity of senile osteoporosis by activating osteocyte autophagy. *Osteoporos Int*. 2016;27(3):1093–1101.
46. **Pietschmann P**, **Skalicky M**, **Kneissel M**, **et al**. Bone structure and metabolism in a rodent model of male senile osteoporosis. *Exp Gerontol*. 2007;42(11):1099–1108.
47. **Kim M-Y**, **Choi H**, **Lee J-H**, **et al**. UV photofunctionalization effect on bone graft in critical one-wall defect around implant: a pilot study in beagle dogs. *Biomed Res Int*. 2016;2016:4385279.
48. **Magat G**, **Oncu E**, **Ozcan S**, **Orhan K**. Comparison of cone-beam computed tomography and digital panoramic radiography for detecting peri-implant alveolar bone changes using trabecular micro-structure analysis. *J Korean Assoc Oral Maxillofac Surg*. 2022;48(1):41–49.
49. **Lee T**. Host tissue response in stem cell therapy. *World J Stem Cells*. 2010;2(4):61–66.
50. **Yamaguchi Y**, **Shiota M**, **Fujii M**, **Shimogishi M**, **Munakata M**. Effects of implant thread design on primary stability-a comparison between single- and double-threaded implants in an artificial bone model. *Int J Implant Dent*. 2020;6(1):42.
51. **Kramer F**, **Voss S**, **Roessig L**, **et al**. Evaluation of high-sensitivity C-reactive protein and uric acid in vericiguat-treated patients with heart failure with reduced ejection fraction. *Eur J Heart Fail*. 2020;22(9):1675–1683.
52. **Xiao W**, **Beibei F**, **Guangsi S**, **et al**. Iron overload increases osteoclastogenesis and aggravates the effects of ovariectomy on bone mass. *J Endocrinol*. 2015;226(3):121–134.
53. **Dong Y**, **Ai C**, **Chen Y**, **et al**. Eph receptor A4 regulates motor neuron ferroptosis in spinal cord ischemia/reperfusion injury in rats. *Neural Regen Res*. 2023;18(10):2219–2228.
54. **Tao Z**, **Tao M**, **Zhou M**, **Wu X-J**. Niacin treatment prevents bone loss in iron overload osteoporotic rats via activation of SIRT1 signaling pathway. *Chem Biol Interact*. 2024;388:110827.
55. **Hua Z**, **Dai S**, **Li S**, **et al**. Deciphering the protective effect of Buzhong Yiqi Decoction on osteoporotic fracture through network pharmacology and experimental validation. *J Orthop Surg Res*. 2023;18(1):86.
56. **Zheng J**, **Jiao S**, **Li Q**, **et al**. Antrodia cinnamomea oligosaccharides suppress lipopolysaccharide-induced inflammation through promoting O-GlcNAcylation and repressing p38/Akt phosphorylation. *Molecules*. 2017;23(1):51.
57. **Bu J**, **Du J**, **Shi L**, **et al**. Eldecalcitol effects on osteoblastic differentiation and function in the presence or absence of osteoclastic bone resorption. *Exp Ther Med*. 2019;18(3):2111–2121.

Author information

Z-S. Tao, MD, Orthopaedic Surgeon,
Department of Orthopedics, The First Affiliated Hospital of Wannan Medical College, Yijishan Hospital, Wuhu, China;
Anhui Province Key Laboratory of Non-coding RNA Basic and Clinical Transformation, Wuhu, China.

C-L. Shen, PhD, Orthopaedic Surgeon, Department of Spinal Surgery, The First Affiliated Hospital of Anhui Medical University, Hefei, China.

Author contributions

Z-S. Tao: Conceptualization, Data curation, Investigation, Project administration, Validation, Writing – original draft.
C-L. Shen: Conceptualization, Investigation, Validation, Writing – review & editing.

Funding statement

The authors disclose receipt of the following financial or material support for the research, authorship, and/or publication of this article: this study was supported by a grant from National Natural Science Foundation of China (82002322) and Health Research Project of Anhui Province (AHWJ2023A20550).

Data sharing

The data that support the findings for this study are available to other researchers from the corresponding author upon reasonable request.

Ethical review statement

The experiment was conducted under the project licence issued according to the institutional guidelines for animal care and use (Approval No. LLSC-2020-082).

Open access funding

The open access fee for this article was self-funded.